Macromolecules

pubs.acs.org/Macromolecules

Article

Bottom-Up Multiscale Approach to Estimate Viscoelastic Properties of Entangled Polymer Melts with High Glass Transition Temperature

Heyi Liang,[§] Kenji Yoshimoto,[*,§] Phwey Gil,[§] Masahiro Kitabata, Umi Yamamoto, and Juan J. de Pablo[*]

Cite This: *Macromolecules* 2022, 55, 3159−3165

Read Online

ACCESS | Metrics & More | Article Recommendations | Supporting Information

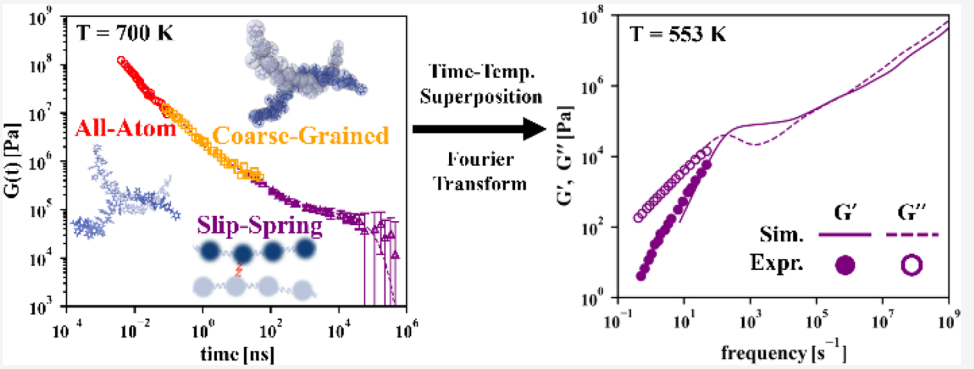

ABSTRACT: A multiscale computational method is presented for the prediction of the viscoelastic properties of entangled homopolymer melts with high glass transition temperatures. Starting from an atomistic model of a polymer, two coarser representations are introduced—a coarse-grained model and a slip-spring representation—which successively operate at longer time and length scales. The three models are unified by renormalizing the time and modulus scales, which is achieved through matching their normalized chain mean squared displacement and stress relaxation modulus, respectively. To facilitate the relaxation of entangled chains, the simulations are performed at temperatures higher than those accessible in experiments. Time−temperature superposition is then applied to extrapolate the viscoelastic properties calculated at high temperatures to experimentally accessible lower temperatures. This proposed approach can predict the linear rheology of the melt starting from an atomistic model and does not require experimental parameters as an input. Here, it is demonstrated for syndiotactic and atactic polystyrene, where good agreement with experimental measurements is observed.

INTRODUCTION

There is a need to develop new polymeric materials that reduce the burden on the environment and help advance efforts toward a sustainable future.[1] Materials informatics strategies can accelerate the design and testing of new polymers. A key consideration for scale-up of such materials into existing equipment and operations is that of processability. In particular, the viscoelastic properties of the melt must be compatible with manufacturing requirements.[2]

The viscoelastic characteristics of polymer melts are a manifestation of molecular relaxation processes that occur over a wide range of time scales. At short time scales, molecules undergo local, segmental motions in a densely packed environment. At longer time scales, molecules slither through one another to diffuse over length scales that exceed characteristic molecular dimensions. These two relaxation processes can be separated by several orders of magnitude in time, depending on the molecular weight and temperature of a melt,[3−5] and cannot be generally bridged by atomistic molecular dynamics (MD) simulations.

Different levels of coarse graining have been proposed to access the broad spectrum of relaxation time of polymers. These include coarse-grained models with different levels of resolution,[6−13] as well as slip-link/slip-spring representations of the material.[14−23] Recently, Behbahani et al. presented a bottom-up multiscale approach that links an all-atom (AA) model to a slip-spring (SS) model by relying on an intermediate scale coarse-grained (CG) representation.[24] Using cis-1,4-polybutadiene (cPB), which has a small Kuhn length, as a model polymer, they were able to predict the shear stress relaxation modulus $G(t)$ of highly entangled cPB melts over the range from 10^{-11} to 10^{-3} s. By integrating $G(t)$, they were also able to estimate the zero-shear viscosity and dynamic

Received: September 29, 2021
Revised: February 9, 2022
Published: April 5, 2022

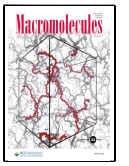

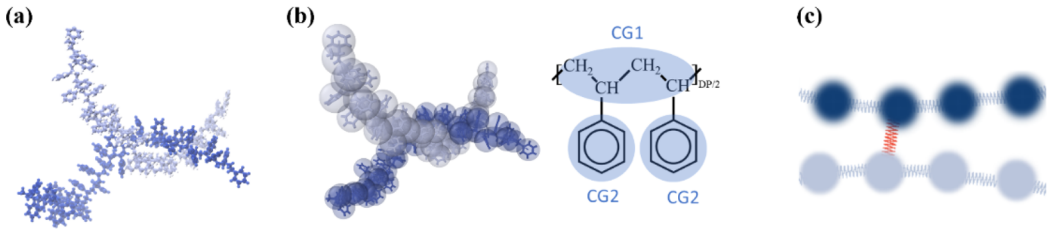

Figure 1. Representation of syndiotactic polystyrene (sPS) with different levels of resolutions. (a) All-atom (AA) model of two sPS segments, each including 30 monomers. (b) Coarse-grained (CG) model mapped from the AA model in (a), and the CG mapping where two consecutive monomers are mapped into three CG beads of two different types (CG1 and CG2). (c) Slip-spring (SS) model of two sPS segments with a SS bond (red) representing an entanglement. Each bead in the SS model represents a sPS segment of about 32 monomers.

moduli of the cPB melt with and without entanglements and found good agreement with experiments. As implemented by Behbahani et al., this multiscale approach was limited to the prediction of viscoelastic properties at a fixed temperature.

In this paper, we introduce a variant of the approach proposed by Behbahani et al. to also predict the temperature-dependent viscoelastic properties of a polymer melt. We focus on syndiotactic polystyrene (sPS), which exhibits a high glass transition temperature and a relatively large persistence length.[25] Due to the high T_g, we choose a considerably high simulation temperature T_{sim} = 700 K to ensure that polymer chains can undergo sufficient relaxation within a limited amount of simulation time. We then adopt a time−temperature superposition principle[5] to estimate the time-shift factor a_T (i.e., the ratio of a viscoelastic property of the sample at temperature T to that at a reference temperature T_0) from atomistic MD simulations of an unentangled sPS melt at different temperatures and extrapolate the viscoelastic properties of the entangled sPS estimated at a higher temperature to lower temperatures using the precalculated a_T. This is based on the assumption that the temperature dependence of the polymer melt dynamics is a direct consequence of different monomer relaxation times.[5] Our approach is rather practical, since many entangled polymer melts exhibit T_g on the order of ∼400 K, leading to significantly slow relaxation dynamics even at the maximum temperature accessible to standard rheology experiments (e.g., ∼500−600 K). This approach can also capture differences in the rheology of polymers having different tacticities, which we demonstrate by comparing results for syndiotactic (sPS) and atactic (aPS) polystyrene.

In what follows, we first discuss the details of the bottom-up multiscale approach and the three models involved, namely, all-atom, coarse-grained, and slip-spring. Second, we construct a master curve for the stress relaxation modulus. Third, we discuss the application of time−temperature superposition for the estimation of the viscoelastic properties of entangled polymer melts. Note that the same approach was adopted for both sPS and aPS. For conciseness, only the sPS is discussed in detail in the abovementioned sections. The details for aPS can be found in the Supporting Information. We conclude with a discussion of the effect of tacticity on the rheology of polystyrene melts.

MODELS AND METHODS

All-atom molecular dynamics (MD) simulations were performed using the standard OPLS-AA force field.[26] To increase computational efficiency, bond lengths between the hydrogen and carbon atoms were constrained with the LINCS algorithm.[27] AA simulations were performed with GROMACS 5.1.4 software.[28,29] We performed simulations of sPS melts with degrees of polymerization (DPs) from 20 to 100 at constant volume and temperature (700 K) to characterize their properties. Additional details about simulation settings and procedures are summarized in the Supporting Information.

The high resolution of the AA model requires considerable computational resources. A lower resolution CG model was therefore used to simulate entangled polymer melts. To construct a CG model, we first applied the graph-based coarse-graining (GBCG) method of Webb et al.[30] to establish the CG mapping of sPS. Briefly, the GBCG method regards a molecule as a graph and creates coarse-grained mappings of controlled resolution by relying on iterative edge contraction. In our CG model, a phenyl group is mapped onto one CG bead, and the backbone CH_2 or CH groups of two monomers are mapped to another CG bead (Figure 1b). At such resolution, the number of simulated particles is reduced from 32 to 3 for two consecutive monomers, while the topological constraints are still preserved (the energy required for backbone bonds to cross each other is ∼150 k_BT at 700 K). The parameters of the CG force field were determined by the iterative Boltzmann inversion (IBI) method with pressure correction.[31] In the IBI method, the CG potential is iteratively updated until various distribution functions (including radial, bond length, bond angle, and dihedral angle distribution functions; see the Supporting Information, Figure S1) match those obtained from the AA model. We performed CG simulations of sPS melts with different DPs from 20 to 600 using LAMMPS[32] at constant volume and temperature (700 K) to characterize their properties. Details of the IBI method, CG force fields, and simulation settings and procedures are provided in the Supporting Information.

At even lower levels of resolution or longer time and length scales, a slip-spring (SS) model was used to describe entangled melts and their rheology. The details of the SS model adopted here have been described in prior publications.[18−21] Briefly, in this model, each particle represents multiple monomers and interacts through a soft potential. Entanglements are described with harmonic interactions between pairs of beads that are referred to as slip-springs. It is a hybrid MC/MD method, which treats the dynamics of the system using MD, while the positions of the slip-springs are evolved with Monte Carlo (MC) moves. The number of slip-springs is controlled by a fugacity[20] $z = \exp(\mu/k_BT)$ in the grand canonical ensemble, where k_B is the Boltzmann constant, T is the temperature, and μ is the pseudo-chemical potential of the slip-springs. Three parameters are required for the SS model: the entanglement molecular weight (i.e., the DP of an entangled segment, N_e), the density ρ, and the chain end-to-end distance R_e. Here, these parameters are extracted from CG simulations of sPS melts with DP = 600. Our simulations yielded ρ = 0.827 g/cm^3 and N_e = 126 using the Z1 algorithm,[33−35] which is close to the experimental result[36] $N_e \approx 140$ and $R_e = 0.788(DP)^{\nu}$ nm. The scaling exponent ν = 0.5 is obtained from CG simulations of sPS melts, and it agrees with the theoretical prediction for chain conformation in the melt (see the Supporting Information, Figure S2). We used $N_{e,ss}$ = 4 beads to represent one entangled segment. Note that our SS model is different from that used by Behbahani et al. with regard to the determination of the fugacity of the slip-springs. In our approach, the fugacity of the slip-spring is fixed at $z = 1/N_{e,ss}$=0.25, while in Behbahani et al., z is adjusted so as to match the

https://doi.org/10.1021/acs.macromol.1c02044
Macromolecules 2022, 55, 3159−3165

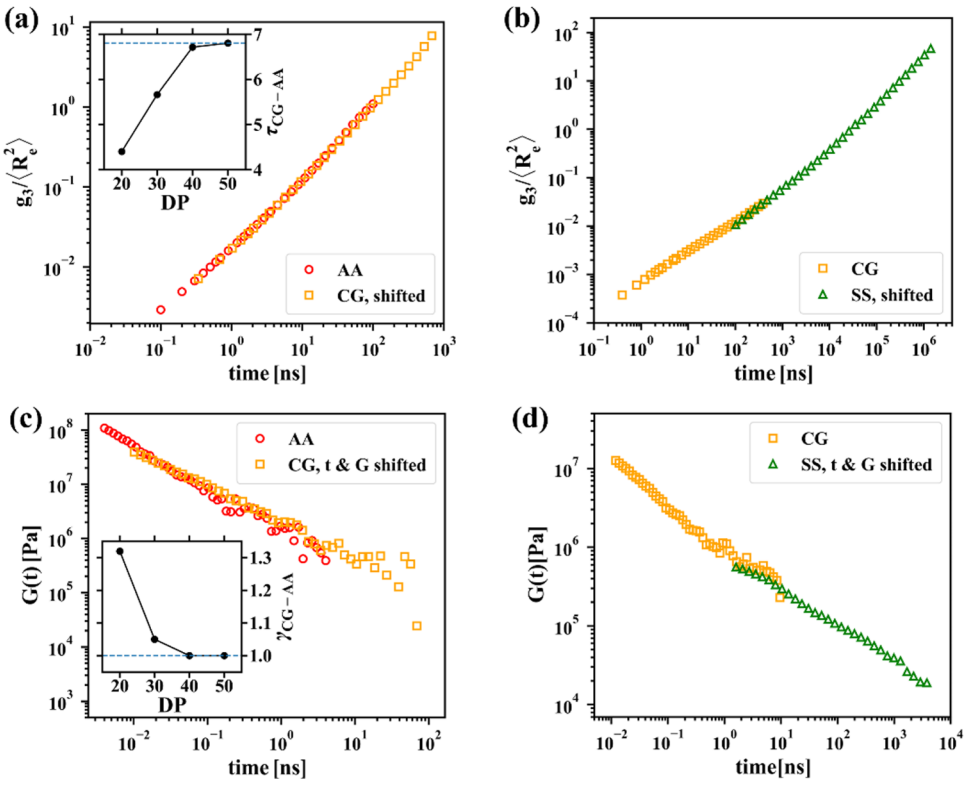

Figure 2. Time and modulus renormalization. (a, b) Normalized chain mean squared displacements of (a) sPS with DP = 50 from all-atom (AA) simulations (red circles) and coarse-grained (CG) simulations with rescaled time (orange squares). (b) sPS with DP = 600 from CG simulations (orange squares) and slip-spring (SS) simulations with rescaled time (green triangles). The CG and SS models overlap in the entanglement region, as shown by the chains' mean-squared displacement data in the Supporting Information, Figure S5 and monomer mean-squared displacement data in the Supporting Information, Figure S6. (c, d) Stress relaxation modulus of (c) sPS with DP = 50 from AA simulations (red circles) and CG simulations with rescaled time and modulus (orange squares) and (d) sPS with DP = 600 from CG simulations (orange squares) and SS simulations with rescaled time and modulus (green triangles). Inset of (a): time renormalization factor as a function of the degree of polymerization. Inset of (c): modulus renormalization factor as a function of the degree of polymerization.

dynamics of the SS model and that of the CG model. Additional details of the simulation settings are discussed in the Supporting Information.

RESULTS AND DISCUSSION

From the aforementioned models, the viscoelastic property of polymer melts can be characterized by the stress relaxation modulus, $G(t)$, which is calculated according to the Green-Kubo relation[37−39]

$$G(t) = \frac{V}{k_B T}\langle \overline{\sigma_{\alpha\beta}}(t)\overline{\sigma_{\alpha\beta}}(0)\rangle \quad (1)$$

where V is the volume of the simulation box, $\overline{\sigma_{\alpha\beta}}(t)$ represent the pre-averaged off-diagonal components of the stress tensor obtained from simulations, and the bracket $\langle ... \rangle$ denotes an ensemble average as well as the average of three off-diagonal components of the stress tensor ($\alpha\beta$ = xy, xz, yz), which is evaluated using a multiple-τ correlator algorithm.[40] The stress relaxation moduli of the AA, CG, and SS models each cover a limited time interval, and they must be "stitched" together to construct a master curve that covers a broader range of time. Note, however, that the stress relaxation modulus obtained from these three models cannot be combined directly due to the following reasons. First, with fewer degrees of freedom, the local friction of a more coarse-grained model is necessarily smaller than that of a model having a higher resolution. The time scales of the CG and SS models must be renormalized to establish a correspondence between these two levels of description. Second, the Hamiltonian of the CG and SS models is different than that of the AA model, and the corresponding moduli must also be renormalized to reach consistency between the elastic energy density of the models.

To match the time scales between the AA and CG models, we compare the normalized chain mean squared displacement (MSD), $g_3/\langle R_e^2\rangle$, of the two models. By normalizing the MSD of the chain center-of-mass, g_3, with the mean squared chain end-to-end distance, $\langle R_e^2\rangle$, we obtain a dimensionless parameter that characterizes the dynamics of the polymer melt. This dimensionless parameter should be independent of the resolution of the model. To match the normalized chain MSD of the CG model to that of the AA model, the CG simulation time is scaled by a factor $\tau_{CG\text{-}AA}$ as shown in Figure 2a. Note that $\tau_{CG\text{-}AA}$ depends on the DP. It increases with increasing DP and saturates at large DPs (see the inset of Figure 2a). This behavior was observed previously in several CG simulations and can be explained by the change of polymer melt density with different DPs due to the additional free-volume of chain ends.[8−10,24] The convergence of $\tau_{CG\text{-}AA}$ indicates that the value $\tau_{CG\text{-}AA}$ = 6.8 at large DPs can be used for longer chains without the need for additional AA simulations. In a similar manner, the time scaling factor for the SS model was determined to be $\tau_{SS\text{-}CG} = 2 \times 10^3$ ns to match its dynamics to that of the CG model as shown in Figure 2b.

https://doi.org/10.1021/acs.macromol.1c02044
Macromolecules 2022, 55, 3159−3165

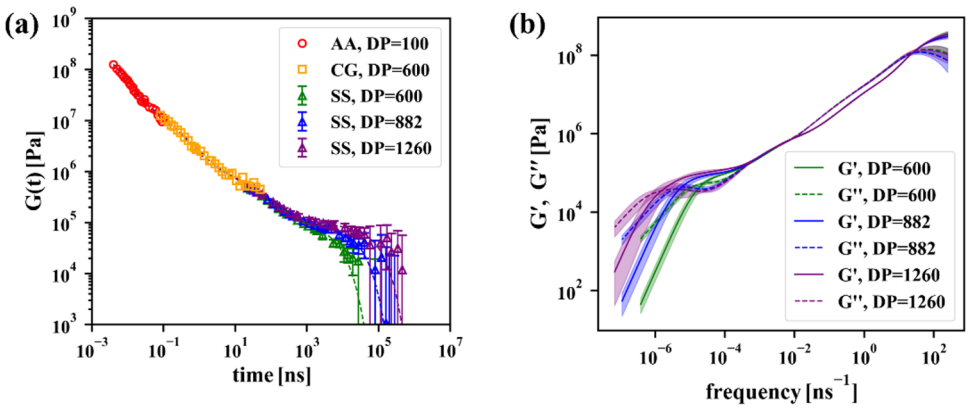

Figure 3. (a) Stress relaxation modulus master curves of entangled sPS melts at 700 K built from all-atom (AA, red circles), coarse-grained (CG, orange squares), and slip-spring (SS, green, blue and purple triangles) models. Error bars of the SS model indicate the uncertainty obtained from six parallel samples. Dashed lines are best fits of the master curve for sPS melt with DP = 600 (green), 882 (blue), and 1260 (purple) using a generalized Maxwell model. (b) Storage (solid lines) and loss (dashed lines) moduli of sPS melt at 700 K with DP = 600 (green), 882 (blue), and 1260 (purple). Shadows indicate the uncertainty obtained from six independent realizations of the simulation.

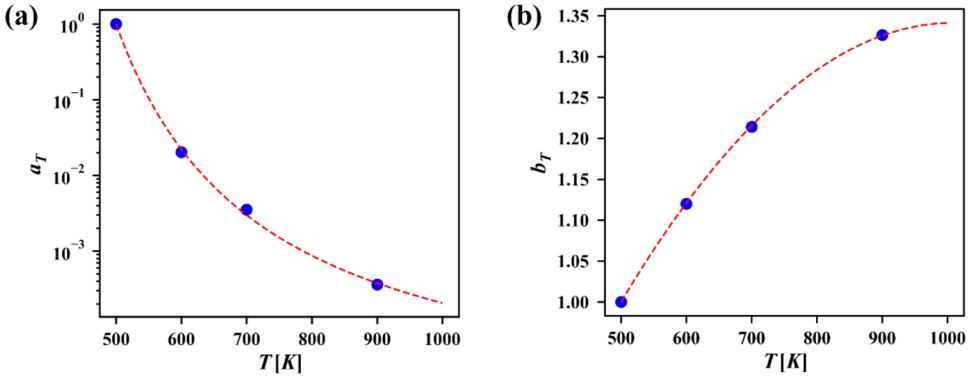

Figure 4. (a) Time-shift factor a_T of sPS as a function of temperature T. The red dashed line corresponds to the best fit of eq 2a with T_0 = 500 K. (b) Modulus-shift factor b_T of sPS as a function of temperature T. The red dashed line corresponds to eq 2b using $\rho(T)/(\mathrm{kg{\cdot}m^{-3}})$ = 1269.4−0.6291 × T/K, T_0 = 500 K and ρ_0 = 954.9 kg·m^{-3}.

To reach consistency between the moduli scales, we compare the stress relaxation moduli of different models. We first scale the time of the CG model by the factor $\tau_{\mathrm{CG\text{-}AA}}$ above. Then, a modulus renormalization factor $\gamma_{\mathrm{CG\text{-}AA}}$ is introduced to bring the CG modulus to match the value of that of the AA model (Figure 2c). Note that $\gamma_{\mathrm{CG\text{-}AA}}$ depends on the DP as well (inset of Figure 2c). It decreases with increasing DP and finally saturates at $\gamma_{\mathrm{CG\text{-}AA}}$ = 1. This means that for CG simulations with longer chains, we need not rescale the modulus. Similarly, to renormalize the modulus of the SS model, we compared the stress relaxation modulus of the CG model to the time-renormalized modulus of the SS model. The modulus scaling factor is $\gamma_{\mathrm{SS\text{-}CG}}$ = 5 × 10^5 Pa, and it is applied to vertically shift its stress relaxation data (Figure 2d). Note that simulated quantities for both the AA and CG models are provided in physical units, while those of the SS model are presented in reduced units (i.e., the units of length, time, and energy are the chain size R_e, reciprocal of the SS bead friction coefficient γ^{-1}, and thermal energy k_BT, respectively; see discussion in the Supporting Information). The scaling factors $\tau_{\mathrm{CG\text{-}AA}}$ and $\gamma_{\mathrm{CG\text{-}AA}}$ are dimensionless, while $\tau_{\mathrm{SS\text{-}CG}}$ and $\gamma_{\mathrm{SS\text{-}CG}}$ have physical units.

To obtain the master curve $G(t)$ of an entangled sPS melt with DP ≫ N_e, it is desirable to calculate the stress relaxation modulus of the same melt from the AA, CG, and SS models. At large DPs, the computational costs of the AA and CG models are significant. Fortunately, for the particular case of sPS and the models that we have adopted here, there is a clear overlap of the short-time stress relaxation moduli at large DPs (see the Supporting Information, Figure S7). At $t \leq 1$ ns, the AA model provides a reliable stress relaxation modulus, which becomes identical at DP = 100. At $t \leq 10$ ns, the stress relaxation modulus of the CG model does not change with DP at DP = 600. This occurs because (i) at time scales shorter than the onset of the entanglement plateau, the stress relaxation modulus reflects the relaxation of short polymer segments, so it does not depend on DP when DP > N_e and (ii) the density of the polymer melt is almost constant at large DPs. Thus, for sPS melts with DP > 600, the master curve can be obtained by combining the stress relaxation modulus from the three models: (i) the AA model with DP = 100; (ii) the CG model with DP = 600, after rescaling the time and modulus by $\tau_{\mathrm{CG\text{-}AA}}$ = 6.8 and $\gamma_{\mathrm{CG\text{-}AA}}$ = 1, respectively; and (iii) the SS model with DP > 600, after rescaling the time and modulus by $\tau_{\mathrm{SS\text{-}AA}} = \tau_{\mathrm{SS\text{-}CG}} \times \tau_{\mathrm{CG\text{-}AA}}$ = 1.36 × 10^4 ns and $\gamma_{\mathrm{SS\text{-}AA}} = \gamma_{\mathrm{SS\text{-}CG}} \times \gamma_{\mathrm{CG\text{-}AA}}$ = 5 × 10^5 Pa, respectively. Figure 3a,b shows the master curve along with the storage and loss moduli of sPS melts with DP = 600, 882, and 1260, where the latter is obtained from the Fourier transform of $G(t)$, which is fitted with a generalized Maxwell model.

To validate the predictions of our multiscale simulations, we now turn to a comparison to experimental measurements. Note that our simulations were conducted at T_{sim} = 700 K, a

https://doi.org/10.1021/acs.macromol.1c02044
Macromolecules 2022, 55, 3159−3165

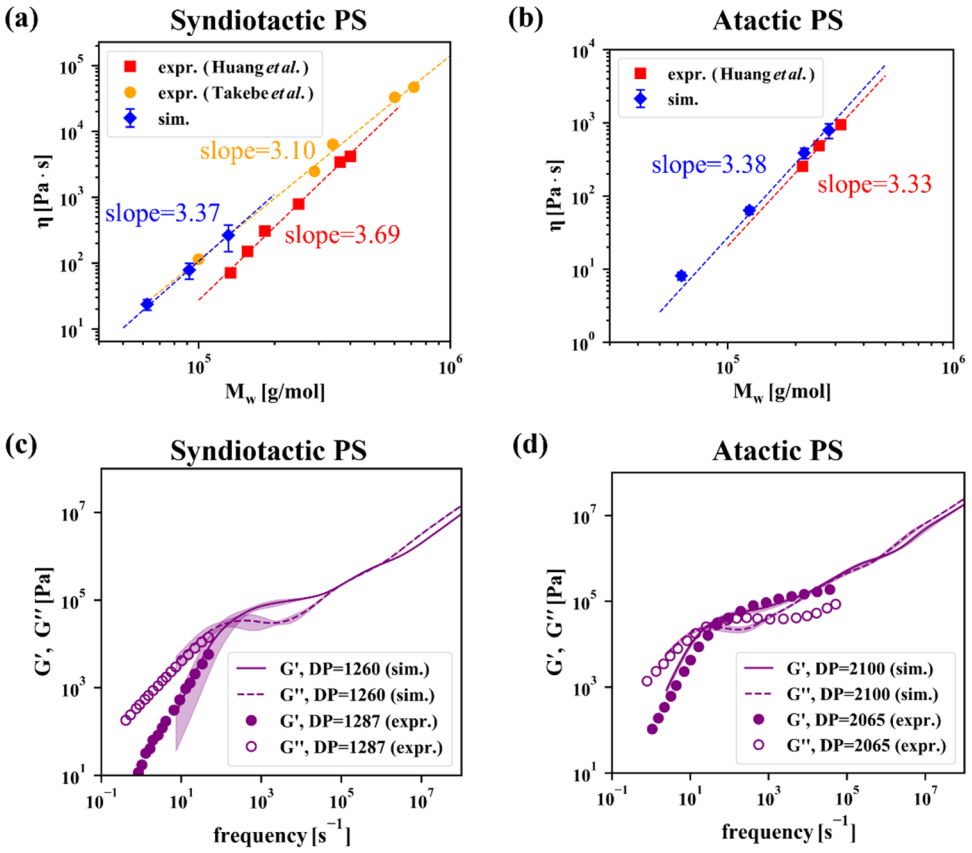

Figure 5. Viscoelastic properties of polystyrene melts at T = 553 K obtained from experiments[36,42] and extrapolated from simulations at T_{sim} = 700 K using time−temperature superposition. (a, b) Viscosity of (a) sPS and (b) aPS as a function of molecular weight. The error bars in the simulation results indicate the uncertainty obtained from six independent realizations of the simulation. (c, d) Storage and loss moduli of (c) sPS melt with DP ≈ 1260 and (d) aPS melt with DP ≈ 2100. Shadows indicate the uncertainty obtained from six independent samples.

temperature that cannot be reached in experiments with sPS. We therefore extrapolate to lower temperature through a time−temperature superposition approach.[5] Specifically, AA simulations of sPS melts with DP = 50 are performed at various temperatures in the range of T = 500−900 K. We then superimpose the stress relaxation modulus at a reference temperature T_0 = 500 K using the time-shift factor a_T and the modulus-shift factor b_T[5,41]

$$a_T(T) = \exp[-c_1(T - T_0)/(c_2 + T - T_0)] \quad (2a)$$

$$b_T(T) = \rho T/\rho_0 T_0 \quad (2b)$$

where $\rho(T)/(\mathrm{kg{\cdot}m^{-3}}) = 1269.4 - 0.6291 \times T/\mathrm{K}$ is the density obtained by fitting the AA simulation results and ρ_0 is the density at the reference temperature. Figure 4a shows the time-shift factor obtained from the AA simulations as well as the best fit by eq 2a, and Figure 4b shows the modulus-shift factor. By applying the resulting a_T and b_T, we can extrapolate our simulation results to any temperature in the range of 500−900 K.

Figure 5a shows a comparison of the experimentally measured zero-shear viscosity of sPS melts of different molecular weights (M_w)[36,42] at T_{expr} = 553 K to the results from the simulations. Note that the viscosity is calculated by integrating the stress relaxation modulus master curve $\eta = \int_0^\infty G(t)dt$. The simulated viscosity at a temperature of T_{sim} = 700 K is extrapolated to T_{expr} = 553 K by multiplying the factor $a_T(T_{expr})b_T(T_{expr})/a_T(T_{sim})b_T(T_{sim})$. The dependence of the zero-shear viscosity of an entangled sPS melt on molecular weight is a power law $\eta \sim M_w^\alpha$, with α = 3.37 from simulations, and α = 3.10 and 3.69 from two different experiments.[36,42] The simulations not only capture the scaling relation between the viscosity and molecular weight, but they are also in quantitative agreement with the experiments. Figure 5c compares the simulation and experiment storage and loss moduli of the sPS melt with almost the same DP ≈ 1260 at 553 K. The experimental results are from Huang et al.,[36] and the viscosity of η = 70 Pa·s is approximately within a factor of 1/3.4 from the simulation result, η = 240 Pa·s. This discrepancy could be due to the high polydispersity of the experimental sample, with a polydispersity index PDI = 1.70. The simulation storage and loss moduli can be extrapolated from T_{sim} = 700 K to T_{expr} = 553 K using the simulated a_T and b_T and are further shifted horizontally by a factor of 3.4 to account for the different viscosity compared to the experiments. The quantitative agreement between the simulation and the experiment serves to underscore the predictive power of the multiscale simulation with the time−temperature superposition strategy adopted here. Note that the comparison of dynamic moduli is limited to the terminal relaxation regime. This is because sPS crystallizes at a relatively high temperature (~530 K),[36] a feature that precludes rheological measurements at lower temperatures (i.e., in a higher frequency regime after time−temperature superposition).

To examine the effect of tacticity on rheology, we also apply the proposed multiscale simulation approach to atactic polystyrene (aPS). Briefly, the atomistic simulations of aPS with DP from 20 to 50 were performed in GROMACS using

https://doi.org/10.1021/acs.macromol.1c02044
Macromolecules 2022, 55, 3159−3165

OPLS-AA force fields at 700 K. In all-atom simulations, aPS chains were generated with random sequences consisting of 50% right-handed and 50% left-handed monomers. Then, the CG model of aPS was built using the same mapping scheme as shown in Figure 1b, and the corresponding CG force fields were derived by iterative Boltzmann inversion (IBI). Note that we did not assign different CG bead types to distinguish PS with different tacticities; however, the effect of tacticity can be captured by the CG force field and manifested in the chain stiffness and entanglement molecular weight. For example, our CG simulations yield $R_e = 0.788(DP)^{0.5}$ nm and $N_e = 126$ for sPS, and $R_e = 0.657(DP)^{0.5}$ nm and $N_e = 180$ for aPS. In the slip-spring model, we used $N_{e,ss} = 3$ beads to represent an entangled strand. Additional details of the simulations and the construction of master curves are provided in the Supporting Information.

Figure 5b compares the zero-shear viscosity of aPS melts of different molecular weights at $T_{expr} = 553$ K from experiments[36] and simulations, which are in quantitative agreement with each other. The viscosity from simulations for syndiotactic polystyrenes, $\eta_{sPS} = 1.5 \times 10^{-15} M_w^{3.37}$(Pa·s), is approximately 5 times higher than that of atactic polystyrene, $\eta_{aPS} = 3.4 \times 10^{-16} M_w^{3.38}$(Pa·s), at the same molecular weight. The entanglement molecular weight of sPS is lower than that of aPS, which is a result of sPS's higher stiffness. A similar effect of tacticity on melt viscosity is observed in the experiments.[36] Figure 5d compares the simulated and experimental storage and loss moduli of the aPS melt with similar molecular weight (DP ≈ 2100) at 553 K. In the terminal relaxation regime (frequency < 10^2 s^{-1}), the simulations and experiments exhibit good agreement. However, in the entanglement regime (10^2 s^{-1} < frequency < 10^5 s^{-1}), the loss modulus obtained from the simulations deviates from that of the experiments. Specifically, the simulated loss modulus shows a sharper and narrower peak near the end of the entanglement regime compared to that found in the experiments. This discrepancy is likely a result of the polydispersity of the experimental samples, a feature that was apparent in earlier experiments.[43] We are currently investigating the polydispersity effects on the dynamic moduli of entangled polymer melts, and the results of that effort will be presented in a future publication.

CONCLUSIONS

To summarize, we have developed a multiscale simulation method to predict the viscoelastic properties (zero-shear viscosity and storage and loss moduli) of polymer melts, using syndiotactic polystyrene as an example. The hierarchical approach involves three models with decreasing resolutions: all-atom, coarse-grained, and slip-spring. The time and modulus scales of models at lower levels of resolution are renormalized by comparing their normalized chain mean squared displacement and stress relaxation moduli to those of the model at higher resolutions. By applying the time–temperature superposition principle, the predicted viscoelastic properties at high simulation temperatures can be extrapolated to lower temperatures, showing reasonable agreement with experimental measurements. In principle, since the proposed method relies only on the availability of an atomistic model to predict the rheology of entangled melts, it could provide a means to computationally screen different materials and to design new polymers with desirable rheological characteristics.

ASSOCIATED CONTENT

Supporting Information

The Supporting Information is available free of charge at https://pubs.acs.org/doi/10.1021/acs.macromol.1c02044.

Simulation details of AA, CG, and SS simulations; chain size from CG simulations; mean squared displacement of chains in CG and SS simulations; monomer mean squared displacement of CG and SS simulations; stress relaxation modulus for AA and CG simulations (PDF)

AUTHOR INFORMATION

Corresponding Authors

Kenji Yoshimoto − *Toray Industries Inc., Otsu, Shiga 520-0842, Japan*; Email: kenji.yoshimoto.z9@mail.toray

Juan J. de Pablo − *Pritzker School of Molecular Engineering, The University of Chicago, Chicago, Illinois 60637, United States*; orcid.org/0000-0002-3526-516X; Email: depablo@uchicago.edu

Authors

Heyi Liang − *Pritzker School of Molecular Engineering, The University of Chicago, Chicago, Illinois 60637, United States*; orcid.org/0000-0002-8308-3547

Phwey Gil − *Pritzker School of Molecular Engineering, The University of Chicago, Chicago, Illinois 60637, United States*

Masahiro Kitabata − *Toray Industries Inc., Otsu, Shiga 520-0842, Japan*; orcid.org/0000-0002-6656-7128

Umi Yamamoto − *Toray Industries Inc., Otsu, Shiga 520-0842, Japan*

Complete contact information is available at: https://pubs.acs.org/10.1021/acs.macromol.1c02044

Author Contributions

[§]H.L., K.Y., and P.G. contributed equally to this work. K.Y., H.L., and P.G. primarily developed the AA, CG, and SS models, respectively. M.K. optimized the AA simulation parameters, and U.Y. aided in interpreting the results. K.Y. and J.J.d.P. conceived of the presented idea and led the work. The manuscript was written through the contributions of all authors.

Notes

The authors declare no competing financial interest.

ACKNOWLEDGMENTS

H.Y. thanks Dr. Ludwig Schneider and Dr. Phillip M. Rauscher for useful discussion and critical reading of the manuscript. K.Y. thanks Prof. Taniguchi for useful discussions. We thank Prof. Abelardo Ramírez-Hernández for discussions regarding slip-spring simulations. Computation time was partially provided by SuperComputer System, Institute for Chemical Research, Kyoto University. This work was supported by Toray Industries. Additional support for the development of software for advanced sampling simulations by the Department of Energy, Basic Energy Sciences, Materials Science and Engineering Division through the Midwest Integrated Center for Computational Materials is is gratefully acknowledged.

REFERENCES

(1) de Pablo, J.; Hillmyer, M.; Buenaflor, J.; Chan, D.; Mysona, J.; Rauscher, P.; Sample, C.; Schneider, L. *Sustainable Polymers Square Table Final Report*; Cambridge University Press & Assessment.

(2) Tadmor, Z.; Gogos, C. G. *Principles of polymer processing*; Wiley: New York, NY, 1997.
(3) de Gennes, P. G. *Scaling Concepts in Polymer Physics*; Cornell University Press: Ithaca, NY, 1979.
(4) Doi, M.; Edwards, S. F. *The Theory of Polymer Dynamics*; Clarendon Press: Oxford, 1986.
(5) Rubinstein, M.; Colby, R. H. *Polymer Physics*; Oxford University Press: New York, NY, 2003.
(6) Faller, R. Automatic coarse graining of polymers. *Polymer* **2004**, *45*, 3869−3876.
(7) Sun, Q.; Faller, R. Systematic coarse-graining of atomistic models for simulation of polymeric systems. *Comput. Chem. Eng.* **2005**, *29*, 2380−2385.
(8) Harmandaris, V. A.; Kremer, K. Dynamics of polystyrene melts through hierarchical multiscale simulations. *Macromolecules* **2009**, *42*, 791−802.
(9) Ohkuma, T.; Kremer, K. Comparison of two coarse-grained models of cis-polyisoprene with and without pressure correction. *Polymer* **2017**, *130*, 88−101.
(10) Salerno, K. M.; Agrawal, A.; Perahia, D.; Grest, G. S. Resolving dynamic properties of polymers through coarse-grained computational studies. *Phys. Rev. Lett.* **2016**, *116*, No. 058302.
(11) Kamio, K.; Moorthi, K.; Theodorou, D. N. Coarse grained end bridging Monte Carlo simulations of poly (ethylene terephthalate) melt. *Macromolecules* **2007**, *40*, 710−722.
(12) Spyriouni, T.; Tzoumanekas, C.; Theodorou, D.; Müller-Plathe, F.; Milano, G. Coarse-grained and reverse-mapped united-atom simulations of long-chain atactic polystyrene melts: Structure, thermodynamic properties, chain conformation, and entanglements. *Macromolecules* **2007**, *40*, 3876−3885.
(13) Song, J.; Hsu, D. D.; Shull, K. R.; Phelan, F. R., Jr.; Douglas, J. F.; Xia, W.; Keten, S. Energy renormalization method for the coarse-graining of polymer viscoelasticity. *Macromolecules* **2018**, *51*, 3818−3827.
(14) Schieber, J. D.; Neergaard, J.; Gupta, S. A full-chain, temporary network model with sliplinks, chain-length fluctuations, chain connectivity and chain stretching. *J. Rheol.* **2003**, *47*, 213−233.
(15) Likhtman, A. E. Single-chain slip-link model of entangled polymers: Simultaneous description of neutron spin− echo, rheology, and diffusion. *Macromolecules* **2005**, *38*, 6128−6139.
(16) Nair, D. M.; Schieber, J. D. Linear viscoelastic predictions of a consistently unconstrained Brownian slip-link model. *Macromolecules* **2006**, *39*, 3386−3397.
(17) Chappa, V. C.; Morse, D. C.; Zippelius, A.; Müller, M. Translationally invariant slip-spring model for entangled polymer dynamics. *Phys. Rev. Lett.* **2012**, *109*, 148302.
(18) Ramírez-Hernández, A.; Detcheverry, F. A.; Peters, B. L.; Chappa, V. C.; Schweizer, K. S.; Müller, M.; de Pablo, J. J. Dynamical simulations of coarse grain polymeric systems: Rouse and entangled dynamics. *Macromolecules* **2013**, *46*, 6287−6299.
(19) Ramírez-Hernández, A.; Müller, M.; de Pablo, J. J. Theoretically informed entangled polymer simulations: linear and non-linear rheology of melts. *Soft Matter* **2013**, *9*, 2030−2036.
(20) Ramírez-Hernández, A.; Peters, B. L.; Andreev, M.; Schieber, J. D.; de Pablo, J. J. A multichain polymer slip-spring model with fluctuating number of entanglements for linear and nonlinear rheology. *J. Chem. Phys.* **2015**, *143*, 243147.
(21) Ramírez-Hernández, A.; Peters, B. L.; Schneider, L.; Andreev, M.; Schieber, J. D.; Müller, M.; de Pablo, J. J. A multi-chain polymer slip-spring model with fluctuating number of entanglements: Density fluctuations, confinement, and phase separation. *J. Chem. Phys.* **2017**, *146*, No. 014903.
(22) Masubuchi, Y.; Langeloth, M.; Böhm, M. C.; Inoue, T.; Müller-Plathe, F. A multichain slip-spring dissipative particle dynamics simulation method for entangled polymer solutions. *Macromolecules* **2016**, *49*, 9186−9191.
(23) Wu, Z.; Milano, G.; Müller-Plathe, F. Combination of hybrid particle-field molecular dynamics and slip-springs for the efficient simulation of coarse-grained polymer models: Static and dynamic properties of polystyrene melts. *J. Chem. Theory Comput.* **2020**, *17*, 474−487.
(24) Behbahani, A. F.; Schneider, L.; Rissanou, A.; Chazirakis, A.; Bačová, P.; Jana, P. K.; Li, W.; Doxastakis, M.; Polińska, P.; Burkhart, C.; Müller, M.; Harmandaris, V. A. Dynamics and rheology of polymer melts via hierarchical atomistic, coarse-grained, and slip-spring simulations. *Macromolecules* **2021**, *54*, 2740−2762.
(25) Malanga, M. Syndiotactic polystyrene materials. *Adv. Mater.* **2000**, *12*, 1869−1872.
(26) Jorgensen, W. L.; Maxwell, D. S.; Tirado-Rives, J. Development and testing of the OPLS all-atom force field on conformational energetics and properties of organic liquids. *J. Am. Chem. Soc.* **1996**, *118*, 11225−11236.
(27) Hess, B.; Bekker, H.; Berendsen, H. J.; Fraaije, J. G. LINCS: a linear constraint solver for molecular simulations. *J. Comput. Chem.* **1997**, *18*, 1463−1472.
(28) Berendsen, H. J.; van der Spoel, D.; van Drunen, R. GROMACS: a message-passing parallel molecular dynamics implementation. *Comput. Phys. Commun.* **1995**, *91*, 43−56.
(29) van der Spoel, D.; Lindahl, E.; Hess, B.; Groenhof, G.; Mark, A. E.; Berendsen, H. J. GROMACS: fast, flexible, and free. *J. Comput. Chem.* **2005**, *26*, 1701−1718.
(30) Webb, M. A.; Delannoy, J.-Y.; de Pablo, J. J. Graph-based approach to systematic molecular coarse-graining. *J. Chem. Theory Comput.* **2019**, *15*, 1199−1208.
(31) Reith, D.; Pütz, M.; Müller-Plathe, F. Deriving effective mesoscale potentials from atomistic simulations. *J. Comput. Chem.* **2003**, *24*, 1624−1636.
(32) Plimpton, S. Fast parallel algorithms for short-range molecular dynamics. *J. Comput. Phys.* **1995**, *117*, 1−19.
(33) Kröger, M. Shortest multiple disconnected path for the analysis of entanglements in two-and three-dimensional polymeric systems. *Comput. Phys. Commun.* **2005**, *168*, 209−232.
(34) Hoy, R. S.; Foteinopoulou, K.; Kröger, M. Topological analysis of polymeric melts: Chain-length effects and fast-converging estimators for entanglement length. *Phys. Rev. E* **2009**, *80*, No. 031803.
(35) Karayiannis, N. C.; Kröger, M. Combined molecular algorithms for the generation, equilibration and topological analysis of entangled polymers: Methodology and performance. *Int. J. Mol. Sci.* **2009**, *10*, 5054−5089.
(36) Huang, C.-L.; Chen, Y.-C.; Hsiao, T.-J.; Tsai, J.-C.; Wang, C. Effect of tacticity on viscoelastic properties of polystyrene. *Macromolecules* **2011**, *44*, 6155−6161.
(37) Green, M. S. Markoff random processes and the statistical mechanics of time-dependent phenomena. II. Irreversible processes in fluids. *J. Chem. Phys.* **1954**, *22*, 398−413.
(38) Kubo, R. Statistical-mechanical theory of irreversible processes. I. General theory and simple applications to magnetic and conduction problems. *J. Phys. Soc. Jpn.* **1957**, *12*, 570−586.
(39) Frenkel, D.; Smit, B. *Understanding Molecular Simulation: from Algorithms to Applications*; Academic Press: New York, NY, 2001.
(40) Ramírez, J.; Sukumaran, S. K.; Vorselaars, B.; Likhtman, A. E. Efficient on the fly calculation of time correlation functions in computer simulations. *J. Chem. Phys.* **2010**, *133*, 154103.
(41) Williams, M. L.; Landel, R. F.; Ferry, J. D. The temperature dependence of relaxation mechanisms in amorphous polymers and other glass-forming liquids. *J. Am. Chem. Soc.* **1955**, *77*, 3701−3707.
(42) Takebe, T.; Yamasaki, K.; Funaki, K.; Malanga, M. Properties of Syndiotactic Polystyrene. In *Syndiotactic Polystyrene: Synthesis, Characterization, Processing, and Applications*; John Wiley & Sons: Hoboken, NJ, 2009; pp. 267−289.
(43) Masuda, T.; Kitagawa, K.; Inoue, T.; Onogi, S. Rheological properties of anionic polystyrenes. II. Dynamic viscoelasticity of blends of narrow-distribution polystyrenes. *Macromolecules* **1970**, *3*, 116−125.

https://doi.org/10.1021/acs.macromol.1c02044
Macromolecules 2022, 55, 3159−3165